500-MB. HEIGHTS AS A LINEAR FUNCTION OF SATELLITE INFRARED RADIATION DATA

CLAYTON E. JENSEN,* JAY S. WINSTON, and V. RAY TAYLOR

National Environmental Satellite Center, Environmental Science Services Administration, Washington, D.C.

ABSTRACT

The technique of stepwise multiple regression is applied to 45 days of data in establishing functional relations between the heights of the 500-mb. surface and TIROS IV long-wave radiation data during the period March to June, 1962. Twenty-six points were selected for height specification in the general area of the eastern Pacific and the North American Continent. Sixty points were selected as a source of radiation "predictors" in a larger area that not only encompasses most of the 26 height points but extends farther westward across the Pacific. Sample charts show the correlation fields that result when the height values at each point are correlated with the radiation data at each of 60 points. The screening process that selects the best predictors is arbitrarily stopped at preset numbers of predictors. The resulting regression equations are evaluated on both dependent and independent samples. Even though the independent results are not outstanding for this particular sample, the method itself appears to offer promise for height and height contour specification over areas where direct measurements of heights are sparse or missing entirely.

1. INTRODUCTION

One of the most important applications of information from meteorological satellites is in the improvement of analyses of surface and upper-air charts. Particularly in data-sparse areas the satellite data could be used as sources of input information for global forecasting models. Subjective adjustments in surface and upper-air analyses have been made with the aid of satellite observations ever since the first TIROS satellite began operating in April 1960. Some examples of the types of analysis modification used in the early days of TIROS data were cited by Winston [12]. In view of the increasing utilization of objective analysis for most large-scale weather maps, the methods of using satellite data must be developed along lines which are as objective as possible. Thus far, in the use of satellite cloud pictures, pure objectivity has been impossible. Recently, however, satellite cloud pictures have been used in a systematic (yet still subjective) fashion to improve the objectively analyzed 500-mb. chart used in operational numerical forecasting (McClain et al. [7]). The results of this work have shown that improvements can be made in forecasts when the initial analysis is adjusted on the basis of satellite information. In pursuing further work along these lines the aim is to develop increasingly more objective methods of applying satellite pictures to reanalysis.

Thus far objectivity has been severely restricted in the use of television pictures since there has been no convenient way to put the information on a purely quantitative basis. However, electronic digitization of picture information (Bristor et al. [1]) will eliminate this restriction commencing with data from ESSA III.

Medium and high resolution radiation data obtained by some TIROS and the Nimbus satellites are quantitative and therefore lend themselves readily to use in an objective manner. Although these data will not be obtainable from the early ESSA satellites, such information should become routinely available within a few years. In particular the scanning radiometer data from a window portion of the infrared spectrum (e.g., 8–12 microns) are especially valuable since they have been shown to reveal clearly the major cloud systems which extend into the middle and upper troposphere (Fritz and Winston [3], Rao and Winston [9], Sherr and Wexler [10], and Widger et al. [11]). These infrared data should prove to be very useful when employed in the type of method developed by McClain et al. [7] for the picture information. However, it is possible that a purely objective, statistical method may be of at least equal value in utilizing the radiation data for improvement of objective analysis.

The present study is a preliminary attempt to determine how well the 500-mb. height field can be specified as a linear function of TIROS IV long-wave radiation data. Since by and large these radiation values are highly correlated with the cloudiness, the investigation depends

*Present affiliation Office of Federal Coordinator for Meteorological Services and Supporting Research, Washington, D.C.

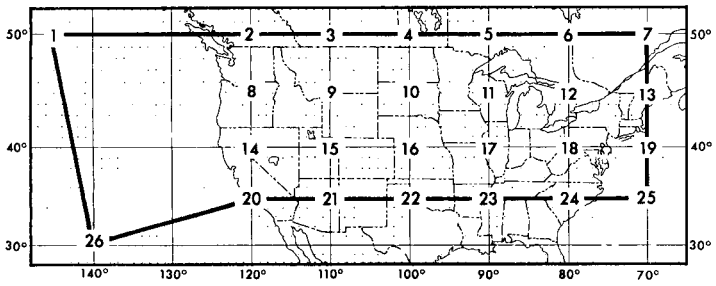

FIGURE 1.—Grid of 26 points at which 500-mb. height data were used for point by point correlations with the radiation field (see fig. 2), and for which heights were specified from resulting regression equations.

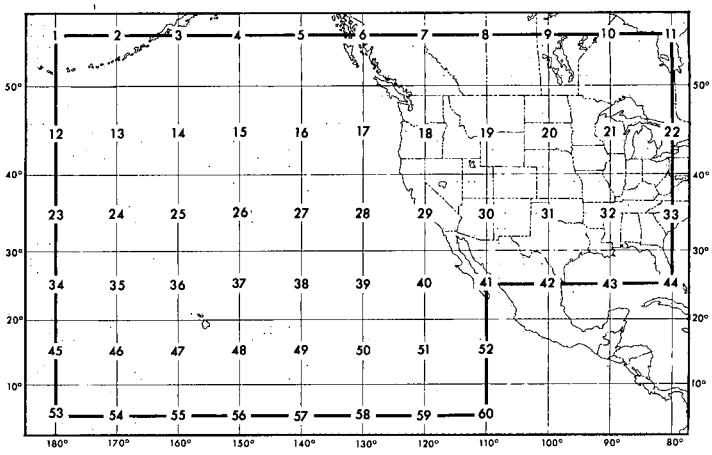

FIGURE 2.—Grid of 60 points at which TIROS IV long-wave radiation data were selected to be used as predictors in specification of heights (see fig. 1).

heavily on how well the broadscale cloud field is correlated with the height field. The screening technique (Miller [8]) is used to derive multiple regression equations that specify the 500-mb. height at a given point as a function of the long-wave radiation data at certain points within a grid whose boundaries may be located several thousand miles away from the point at which heights are being specified. This is essentially the same procedure applied by Klein [4] in trying to solve the inverse problem of specifying cloudiness and precipitation as a function of the mid-tropospheric height field. Although the primary objective of this work is to see how well the height field can be specified by the radiation field, the spatial correlation fields obtained between heights and radiation over a large area can be very instructive in revealing the broadscale relationship of major cloud systems to the mid-tropospheric flow. This should aid in the better understanding of the physical relationships between the flow pattern and the cloud field.

2. DATA

From a total of approximately 120 days of radiation data coverage by TIROS IV, 45 days were selected on the basis of high density of radiation data over North America and the Pacific Ocean and of closeness in time of the data to 0000 GMT, the time of the height observations used. The radiation data were derived from composite daily maps prepared at the National Environmental Satellite Center from channel 2 data (8–12 microns) of the TIROS IV satellite. In these composite maps radiation measurements from each day of TIROS IV observations were averaged over 5° latitude-longitude boxes and assigned to grid points. (More details about the derivation of these data may be found in [13].) 500-mb. heights were obtained by interpolation of the objectively analyzed data of the National Meteorological Center.

Figure 1 shows the positions of the 26 points, numbered as indicated, at which heights at 500 mb. were to be specified. Twenty-four points were chosen because they lie in a dense data region over North America where observed heights are highly reliable. Two grid points were also selected over the eastern Pacific Ocean, located at weather ships N and P so that observed heights would have relatively small errors for an ocean region.

Figure 2 shows the positions of the 60 points, numbered as indicated, at which values of outgoing long-wave radiation were determined. These points do not extend north of 55°N. because of lack of coverage by the TIROS IV satellite in its particular orbit. Radiation data from the western Atlantic are very sparse since radiation values obtained during interrogation of the satellite by the east coast command and data acquisition station have been unavailable. Admittedly the lack of data from northern Canada, Alaska, and the western Atlantic is a severe restriction, particularly for specifying heights over the eastern half of the United States. This emphasizes the preliminary nature of this study.

TABLE 1.—*List of 45 days used in this study with corresponding calendar dates and time intervals over which radiation data were acquired.*

Day After Launch	Dates 1962	Time (GMT) From	Time (GMT) To	Day After Launch	Dates 1962	Time (GMT) From	Time (GMT) To
37	Mar. 17–18	2055	0717	95	May 14	0123	1322
38	Mar. 18–19	2350	1004	96	May 15	0046	1246
39	Mar. 19–20	1941	0927	97	May 16–17	2332	1317
40	Mar. 20–21	2050	0851	98	May 17–18	2258	1241
41	Mar. 21–22	2158	0814	99	May 18–19	2222	0842
42	Mar. 22–23	1937	0410	100	May 19–20	2325	0806
43	Mar. 23–24	1903	0702	101	May 20–21	2253	0729
44	Mar. 24–25	1913	0808	102	May 21–22	2217	1016
45	Mar. 25–26	1749	0733	103	May 22–23	2156	0800
46	Mar. 26–27	1918	0658	104	May 23–24	2104	0724
50	Mar. 30–31	1829	0252	105	May 24–25	2027	0826
51	Mar. 31–Apr. 1	1554	0539	106	May 25–26	1950	0935
52	Apr. 1–2	1518	0317	107	May 26–27	2006	0858
53	Apr. 2–3	1625	0103	108	May 27–28	1840	0824
54	Apr. 3–4	1719	0349	111	May 30–31	1832	0817
55	Apr. 4–5	1525	1314	112	May 31–June 1	1755	0740
56	Apr. 5–6	1550	0421	113	June 1–2	1904	0519
57	Apr. 6–7	1544	0022	114	June 2–3	1643	0627
58	Apr. 7	1842	2343	115	June 3–4	1606	0225
61	Apr. 10	1319	2333	117	June 5–6	1637	0622
62	Apr. 11–12	1240	0040	118	June 6–7	1603	0546
63	Apr. 12–13	1323	0148	119	June 7–8	1631	0510
65	Apr. 14–15	1054	0038				

In order to insure a reasonable sample of radiation data, even for the points shown in figure 2, interpolation or extrapolation of data was necessary in some instances to fill out the grid of 60 points, particularly near the borders. The 45 days selected have calendar dates ranging from March 17 to June 8, 1962. Table 1 lists the 45 days of radiation data used with the time period within which data were acquired.

From point-by-point listings of the data which were used in this study, seasonal trends in both height and radiation were noted. In order to eliminate the bias of seasonal trends, data at each point were adjusted before the correlation fields were constructed. The magnitude and direction of the seasonal trend for a particular point seemed mostly to be a function of its latitude and its position over land or ocean. Correlation fields constructed without removal of the seasonal trends verified the existence of a bias, usually in the positive direction.

3. CORRELATION FIELDS

Simple linear correlation coefficients between 500-mb. heights at each of the 26 height points and the long-wave radiation values observed on the same occasions over the 45 days at each of the 60 radiaton points were computed, plotted, and analyzed. An additional grid of 60 radiation points, shifted 5° longitude west of those in figure 2, was used to check ambiguities in the analyses and more closely locate and determine the magnitudes of maxima and minima. Sample charts of correlation fields are shown in figures 3–8 for height points numbered 1, 14, 15, 16, 17, and 26, respectively. From a statistical significance test using Student's t distribution, for the population size involved here, significance at the 10 percent level or better is indicated by a correlation coefficient whose absolute magnitude is 0.25 or greater. This significance level may be optimistic since account was not taken of the possible effects of successive data being positively correlated. It is given merely as a level below which the analysis of the correlation fields would have little meaning. The placement of the zero line must be considered as somewhat arbitrary.

In figure 3 it is found that the highest positive correlations lie in an elongated northeast-southwest band to the east and south of height point 1. This pattern indicates that low heights at 500 mb. are associated with low values of outgoing radiation (i.e., major cloudiness extending to the middle and upper troposphere) to the east and south. This is consistent with the synoptic climatology of a 500-mb. trough in the vicinity of point 1. Conversely, high 500-mb. heights at point 1 are associated with concurrent high values of outgoing radiation (clear to scattered clouds) to the east and south. A region of negative correlation is located with a similar orientation in the vicinity of point 1 and to the west. This indicates that when heights are low at point 1 the radiation immediately

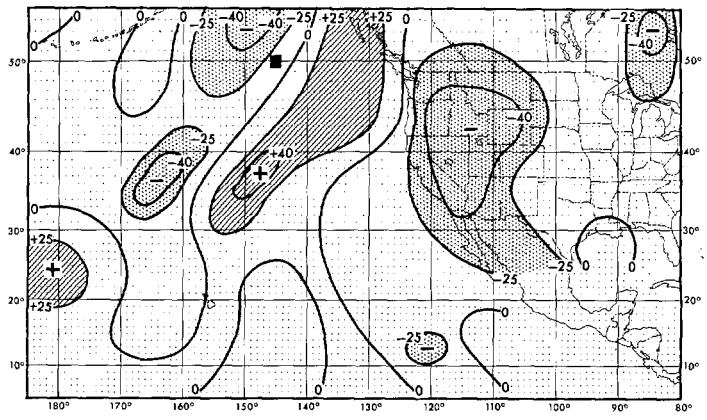

FIGURE 3.—Simple linear correlation field between D-values of 500-mb. height at point 1 (located by black square) and concurrent long-wave radiation data from field covered by points in figure 2 for 45 cases. Values are in percent.

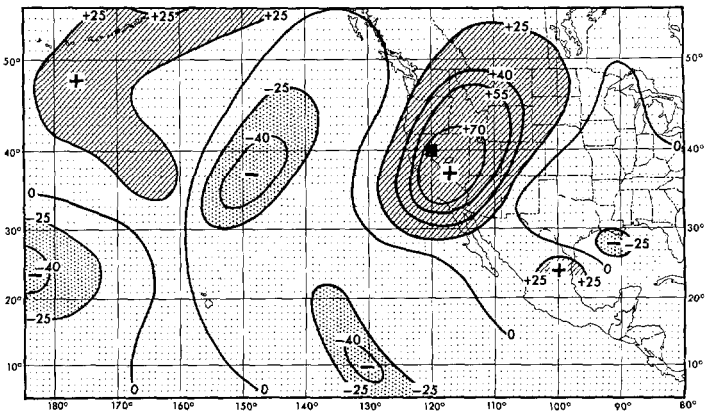

FIGURE 4.—Simple linear correlation field between D-values of 500-mb. height at point 14 (located by black square) and concurrent long-wave radiation data from field covered by points in figure 2 for 45 cases. Values are in percent.

to the west tends to be relatively high since clouds generally are low or are scattered to broken to the rear of the trough. For higher heights at point 1 the radiation tends to be low to the west and hence more cloudiness extending to higher levels exists.

It is interesting that high negative correlations are also found over a large region of the western United States. Relationships involving such great distances are undoubtedly related to the large-scale wave pattern with a half wavelength on the order of 30° longitude in this region. In other words, if a trough is located well off the Pacific coast in the spring, in the neighborhood of ship P, the ridge downstream is likely to be near the west coast. The tendency would then be for relatively little cloudiness and high radiation over most of the western States. The situation with a ridge near ship P would essentially be the opposite of the trough case.

Next, for height point 14 on the California-Nevada

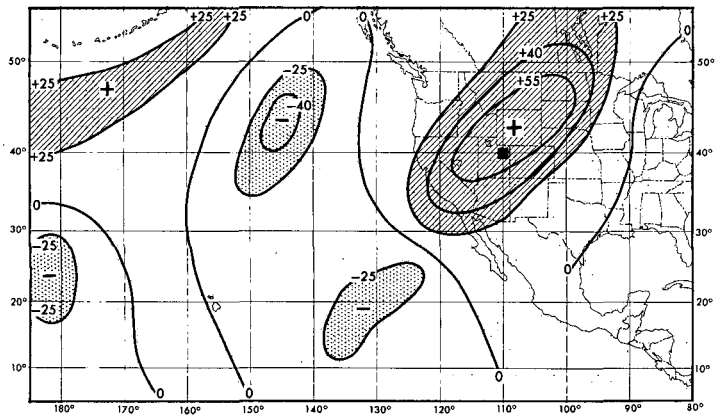

FIGURE 5.—Simple linear correlation field between D-values of 500-mb. height at point 15 (located by black square) and concurrent long-wave radiation data from field covered by points in figure 2 for 45 cases. Values are in percent.

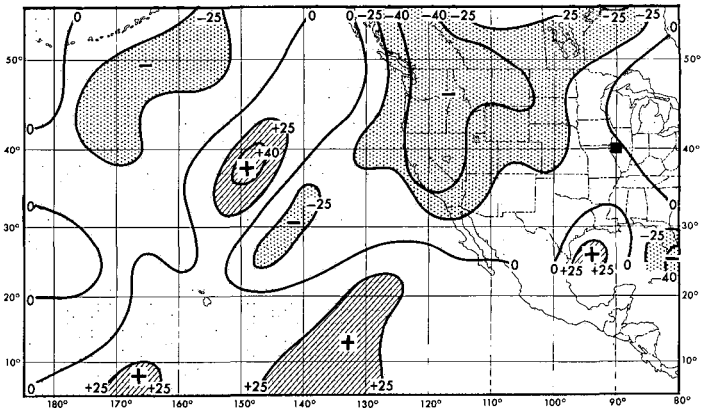

FIGURE 7.—Simple linear correlation field between D-values of 500-mb. height at point 17 (located by black square) and concurrent long-wave radiation data from field covered by points in figure 2 for 45 cases. Values are in percent.

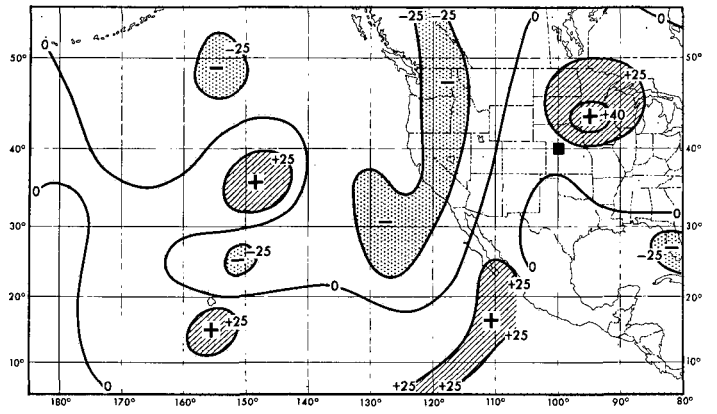

FIGURE 6.—Simple linear correlation field between D-values of 500-mb. height at point 16 (located by black square) and concurrent long-wave radiation data from field covered by points in figure 2 for 45 cases. Values are in percent.

border (fig. 4), it is seen that the region of highest positive correlation is again to the east and southeast of the height point, much stronger, and somewhat closer to the point, than in figure 3, suggesting that the wave pattern and the associated cloudiness (or low outgoing radiation) are also closer together over the western United States. As in the case of ship P (fig. 3), figure 4 suggests a wave pattern with negative correlations located at about 30° longitude both east and west of point 14.

It is interesting also that some larger correlations, both positive and negative show up in the Pacific, some 50°–60° of longitude from the west coast. Since the radiation data grid remains fixed throughout this study, it is not possible to determine whether such correlations exist at a similar distance westward from point 1. Likewise, of course, it cannot be said what relationships may exist at a similar distance to the east of point 14.

Figure 4 in a broad sense has a similar appearance to figure 3, with the stronger correlations reversed in sign. This is to be expected since the point of reference has been shifted one-half wavelength to the east.

For point 15 the area of highest positive correlation has its axis very nearly through the height point (fig. 5). This essentially indicates that the 500-mb. wave pattern and the cloudiness are nearly superimposed. The remainder of the pattern in figure 5 over the Pacific area shows considerable similarity to the correlation distribution in figure 4, including the relatively high negative correlations in the central Pacific (i.e., near the lower left edge of the map).

Figure 6 shows a striking change in the correlation patterns as the height point of reference is shifted east of the Rockies to the Central Plains. The area of strongest positive correlations in this case is north and east of the height point and lacks the northeast-southwest orientation which was present in the previous correlation fields. This is very likely indicative of the usual relationship between cloudiness in this part of the country and the trough and ridge systems. In fact, the general orientation of cloudiness relative to the trough location as indicated by the positive correlation area in figure 6 loosely resembles the general distribution of the precipitation area associated with Colorado cyclogenesis in the spring as shown by Fawcett and Saylor [2]. Also the general change in relative position of the height point and the maximum correlation as the point of reference is moved eastward from the west coast into the central United States is similar to the changes in relative positions found by Klein [4] and Klein et al. [5] in their studies of precipitation and cloudiness as functions of the height field.

Figure 7 resembles figure 3 over much of the area shown. The reference point (No. 17) is located very nearly 60° east of ship P. This probably means that points 1 and 17 are at a distance of essentially one wavelength in both height and cloud fields at this time of year. Or in other words, a trough (ridge) in the central United States is usually accompanied by a trough (ridge) in the eastern Pacific in the spring.

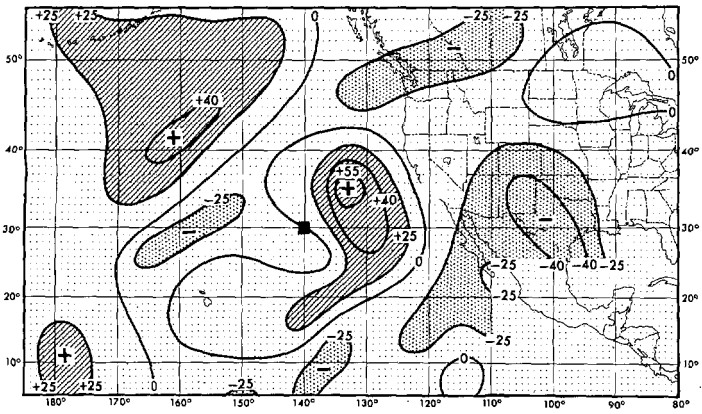

FIGURE 8.—Simple linear correlation field between D-values of 500-mb. height at point 26 (located by black square) and concurrent long-wave radiation data from field covered by points in figure 2 for 45 cases. Values are in percent.

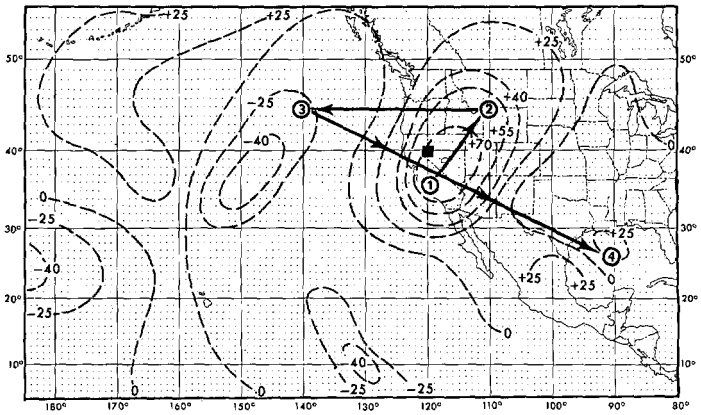

FIGURE 9.—Positions of four radiation predictors in order chosen for specification of height at point 14. Regression field of figure 4 is reproduced in dashed lines for comparison.

There is some indication that an area of significant positive correlation exists east of point 17 as in the case of other points farther to the west. However, the lack of radiation data along and off the east coast required termination of the radiation data grid at 80° W., so correlations farther east of point 17 are indeterminable for the present.

The correlation field for point 26 (fig. 8) is of some interest relative to the other oceanic point farther north (point 1—fig. 3). The area of positive correlation to the east extends from northeast through east, then south of the point. This differs markedly from the nearly straight northeast-southwest orientation of the positive area associated with point 1 and also lacks the strong negative area to the northwest. If one considers this pattern, including the minimum correlation immediately south of point 26, it very much resembles the type of cloud cover associated with closed low centers, where the major cloud system is mainly concentrated to the northeast, but extends in a spiral shape around the center. This suggests that when heights are low at point 26 there is generally a closed cyclonic center nearby, whereas at point 1 low heights are usually associated with an extensive north-south trough. The spiral pattern also would be consistent with the higher height values at this point, if most of the highest heights occur with closed anticyclonic centers at 500 mb. Minimum major cloudiness would be expected around an anticyclone's northeast and east sides and possibly extending southward in an anticyclonic spiral pattern. It must be pointed out, however, that the spiral cloud patterns have shown up in most clearcut fashion for low centers in the pictures and radiation data from satellites.

Other portions of the correlation field for point 26 show varying amount of resemblance to the field for point 1. The region of negative correlations some 30°–40° longitude to the east is somewhat similar. To the northwest of point 26 there is a relatively strong maximum of positive correlation. Whether a counterpart of this exists relative to point 1 cannot be said, since such an area is outside the area of radiation data used.

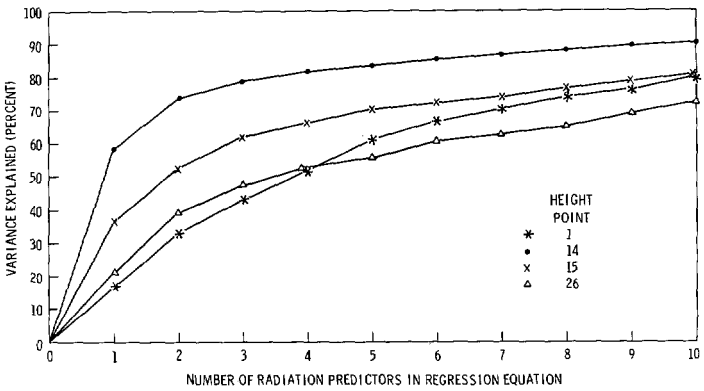

FIGURE 10.—Percentage of variance explained by regression equations for selected height points (see fig. 1), involving various numbers of radiation predictors.

4. REGRESSION ANALYSIS FOR DEPENDENT DATA

Stepwise multiple regression was used in a computer program to generate a regression equation for each of the 26 height points. A sample of such an equation having four radiation points as "predictors" is

$$H(14) = -0.7145 + 3.4010R(29) + 1.3285R(19) - 1.4046R(16) - 0.7902R(43) \quad (1)$$

where the number in parentheses on the left refers to a particular height point (No. 14) in the set of 26, and the numbers in parentheses on the right side of the equation refer to the particular radiation points that were selected from the 60-point grid in the screening process. Height values are in units of kilometers and represent a departure from the standard atmosphere 500-mb. height of 5.570 km. (D-value). Radiation values, in units of ly./min., are adjusted, as in the construction of the correlation fields, to remove the seasonal trend. Resulting specified heights

must then be adjusted in the reverse manner (i.e., put back seasonal trend in heights) in order to be compared with observed heights.

Figure 9 shows the locations of the four radiation points that were selected in equation (1) above for point 14. (The correlation field of fig. 4 has been duplicated in dashed lines.) The percentage of the non-seasonal variance of the height at point 14 explained by the specification equation (1), based on the field of concurrent long-wave radiation data, is 81.4 percent. Figure 10 shows the relationship between the amount of variance explained and the number of predictors chosen for several selected height points. In order to choose a close to optimum number of predictors, consideration had to be made that the regression equations involved were to be applied both to dependent height specifications and later to independent height specifications. In this regard we were guided by the work of Lorenz [6] and especially his observation that difficulties arise when the ratio of number of predictors to sample size is large. The trouble lies in the desire to introduce a great many predictors to increase the reduction in variance within the original sample. The risk is that with the greater number of predictors, there will be a greater probability that some linear combination of these predictors will be correlated with the predictand within the sample, even though it may be uncorrelated with the predictand within the population. Thus, too many predictors will probably increase the error when the regression equation is applied to independent data. Figure 10 shows that the gain in the amount of variance explained by using more than four predictors is small, and so this number was arbitrarily chosen to compute the height fields which are shown here.

Regression equations utilizing four radiation points as predictors were obtained at the 26 height points for the 45 cases at hand and applied to dependent data. Figures 11a–14a illustrate specified height fields for four days at 0000 GMT based upon radiation data for March 23–24, April 4–5, May 24–25, and May 27–28 respectively. Figures 11b–14b are the observed height fields for 0000 GMT on these same days.

It can be seen that the height contour specification is reasonably good for all four days shown. Height contour specifications for nine other days of the whole set of 45 were also analyzed, and with one exception (April 14–15) resemble the actual height fields about as well as the four days shown. For April 14–15, root mean square errors in height specification were about twice as large as for any of the other days that were used.

Each of the four days shown illustrates a different pattern of flow, especially over the western half of the United States: a Rocky Mountain trough (fig. 11), a Rocky Mountain ridge (fig. 12), a large closed Low west of the Rockies (fig. 13), and an open trough over most of the West (fig. 14). It would seem that the degree of success obtained in specifying height contours with the

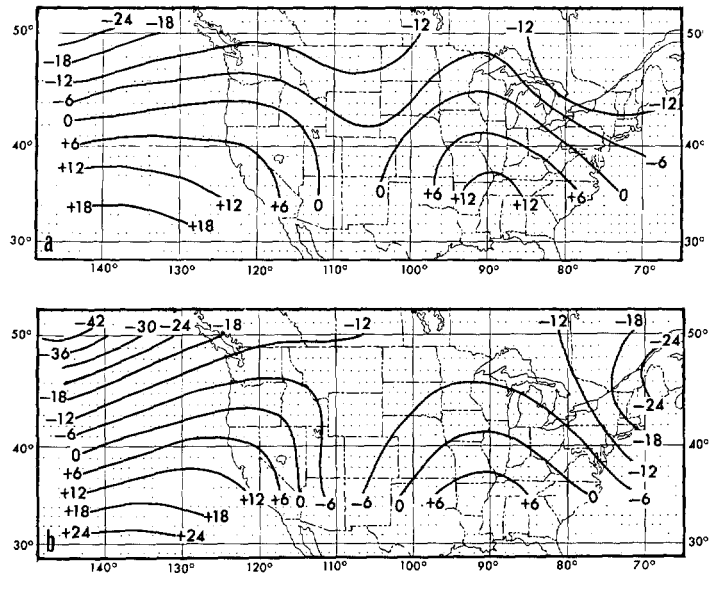

FIGURE 11.—Specified (a) and observed (b) 500-mb. height fields for 0000 GMT, March 24, 1962. (a) is based upon radiation data for TIROS IV, day 43, computed by regression equations obtained from 45 cases including day 43 and using 4 predictors. Heights are *D*-values from standard atmosphere in 10's of meters.

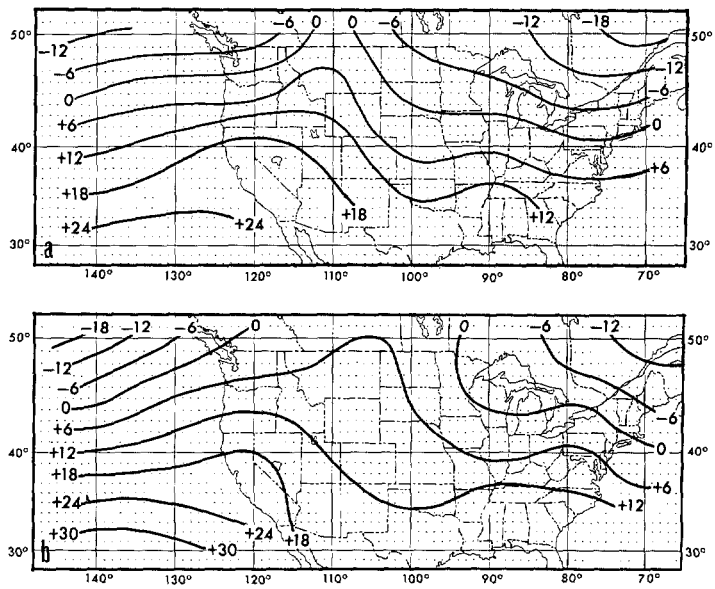

FIGURE 12.—Specified (a) and observed (b) 500-mb. height fields for 0000 GMT, April 5, 1962. (a) is based upon radiation data for TIROS IV, day 55 computed by regression equations obtained from 45 cases including day 55 and using 4 predictors. Heights are *D*-values from standard atmosphere in 10's of meters.

set of regression equations is not dependent on a predominance of high or low radiation values.

In order to specify height fields for independent days, and to check the effect on the dependent days of reducing an already small population, regression equations were obtained for a subset of the original 45 days consisting

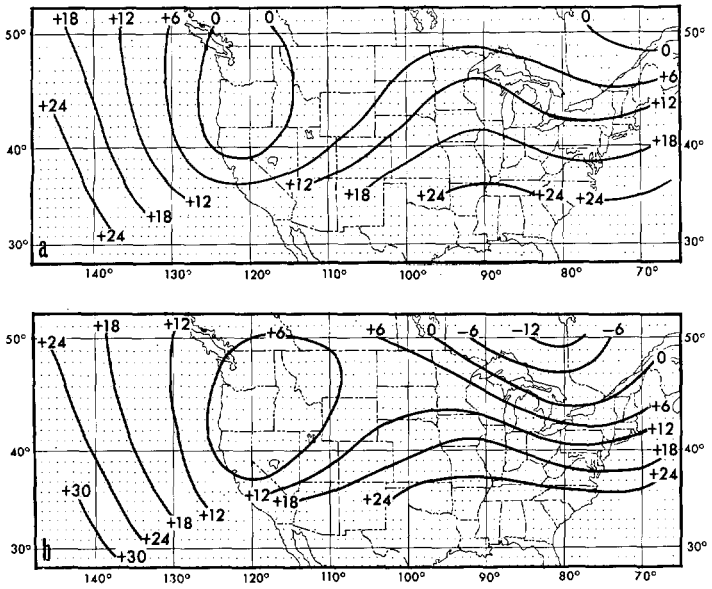

FIGURE 13.—Specified (a) and observed (b) 500-mb. height fields for 0000 GMT, May 25, 1962. (a) is based upon radiation data for TIROS IV, day 105 computed by regression equations obtained from 45 cases including day 105 and using 4 predictors. Heights are D-values from standard atmosphere in 10's of meters.

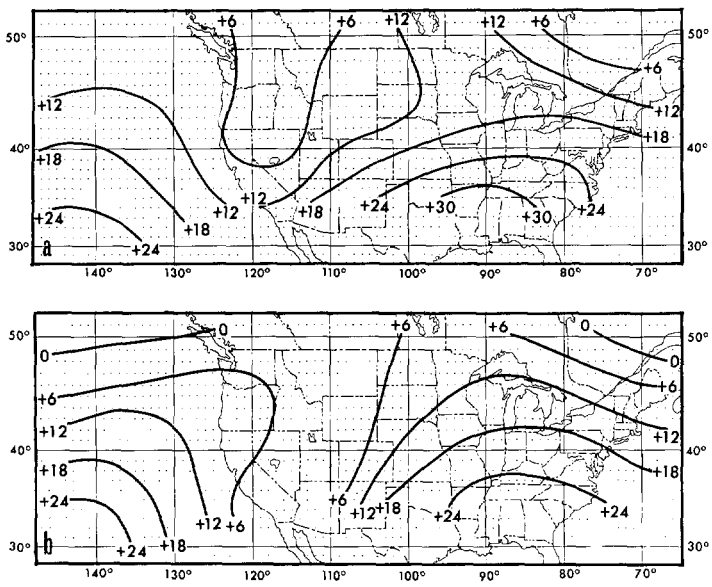

FIGURE 14.—Specified (a) and observed (b) 500-mb. height fields for 0000 GMT, May 28, 1962. (a) is based upon radiation data for TIROS IV, day 108 computed by regression equations obtained from 45 cases including day 108 and using 4 predictors. Heights are D-values from standard atmosphere in 10's of meters.

of 42. Also to check further the effect of varying the number of predictors used in the regression equations, equations using 4 and 6 predictors were obtained. Means and standard deviations of actual heights and specified heights are given in table 2 along with the root mean squares of the differences. Dependent specifications are

TABLE 2.—*Statistics of observed and specified 500-mb. heights for selected days. The first four days shown (43, 55, 105, 108) are those whose contours are shown in figures 11–14. The remaining days, 45 and 65, along with 115, whose contours are shown in figure 12, are those for which independent specifications were made. Errors are the root mean squares of differences between observed and specified heights. All units are in km. Mean heights represent departures from the standard atmosphere 500-mb. height of 5.570 km.*

OBSERVED			SPECIFIED							
				45 Cases			42 Cases			
Day	Mean	Standard Deviation	Number of Predictors	Mean	Standard Deviation	Error	Mean	Standard Deviation	Error	
43	−0.067	0.130	4	−0.041	0.115	0.054	−0.040	0.119	0.062	DEPENDENT
			6	−.048	.122	.045	−.046	.128	.050	
55	.056	.113	4	.030	.127	.055	.029	.130	.060	
			6	.031	.134	.052	.034	.132	.055	
105	.107	.117	4	.108	.098	.057	.111	.103	.062	
			6	.116	.102	.056	.111	.103	.054	
108	.108	.092	4	.143	.084	.051	.141	.100	.054	
			6	.141	.035	.051	.143	.094	.057	
45	.012	.109	4	.012	.108	.050	.012	.108	.095	INDEPENDENT
			6	.022	.105	.058	.022	.105	.088	
65	−.001	.218	4	.050	.123	.015	.050	.123	.178	
			6	.043	.137	.100	.043	.137	.185	
115	.150	.111	4	.144	.096	.062	.144	.096	.104	
			6	.147	.094	.042	.147	.094	.097	
				DEPENDENT			INDEPENDENT			

shown for seven days which include the four days mentioned previously. The larger population and greater number of predictors appear to give the best results, but differences are small and not very significant.

5. REGRESSION ANALYSIS FOR INDEPENDENT DATA

The last three days shown in table 2, i.e., March 24–25, 1962, April 14–15, 1962, and June 3–4, 1962 (days 45, 65, and 115 after launch), were randomly withheld from the original set of 45 cases. The regression equations derived from the remaining 42 cases were applied to these days to give independent specifications of height. A sample equation that may be compared with (1) is

$$H(14) = -0.5803 + 3.6053R(29) + 0.9480R(19) - 1.4235R(16) - 1.0739R(43) \quad (2)$$

It can be seen that the independent results (set of 42 cases) have height errors that are significantly larger than the errors for the dependent results. A height contour field for one of the independent days (March 26) is shown in figure 15a. Some resemblance to the actual height field (fig. 15c) and to the dependent field (fig. 15b) can be seen, even though the specification of absolute heights at certain individual points is very poor.

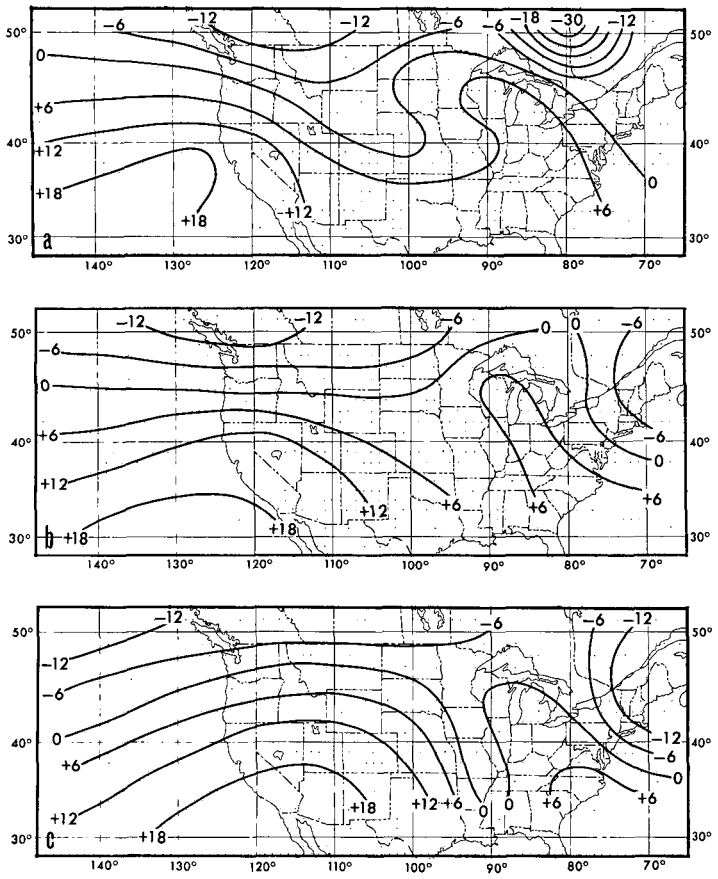

FIGURE 15.—Specified (a) and (b), and observed (c) 500-mb. height fields for 0000 GMT, March 26, 1962 (TIROS IV, day 45). (a) is an independent specification made with equations obtained from 42 cases not including day 45. (b) is a dependent specification made with equations obtained from 45 cases which include day 45. Equations for both (a) and (b) use 4 radiation predictors. Heights are *D*-values from standard atmosphere in 10's of meters.

6. CONCLUSION

The method of specification of 500-mb. heights which has been described here, appears to be promising. Of course, the study must be considered quite preliminary since the sample of 45 cases is small and there were rather severe restrictions on the area over which data were available. The statistics shown in table 2 would be improved if the error contribution of points near the eastern edge of the area were neglected. The regression equations for such points appear somewhat less reliable than those for points farther west, since it was impossible to consider predictors in the western Atlantic. A further contribution to the specification errors arises from the proximity of the eastern and northern height points to the edges of the radiation data area where data are somewhat limited. With increased data coverage and reliability available with future satellites, it is hopefully anticipated that such specification of 500-mb. height from the radiation field will be put on a more reliable basis.

Although the absolute 500-mb. height values specified by the regression equations using dependent data contain fairly large discrepancies in some cases, the resulting contours compare well with the observed patterns for the most part. This suggests that a useful application of the satellite long-wave radiation data in the context of this study might be more as an indicator of the presence or absence of troughs and ridges with accompanying wind flow than as a precise specifier of absolute heights. For certain areas, however, i.e., portions of the western United States, even absolute height was well indicated for almost all the 13 dependent and 3 independent cases which were examined.

The application of this regression method to specify 500-mb. heights in areas of sparse data would have to be carried out by assuming that the fields of correlation and the regression equations, derived for points that are well observed with radiosondes or other conventional means, will hold for other regions of similar synoptic climatology where data are sparse. These equations could then be transferred to the data-sparse regions, keeping the grids fixed relative to the points involved. This is probably not feasible with the data we now have and would thus have to wait until relationships are established over much larger areas in the future. If this transferral is possible, then these regression methods could be utilized to improve the height analyses in sparse data areas, providing that long-wave radiation data from weather satellites are available over a considerable area surrounding the region in which improvements are to be made.

ACKNOWLEDGMENTS

The authors are indebted to Mr. Frank Lewis for furnishing the computer program that accomplished the stepwise multiple regression analysis. In addition, thanks are due to Mr. Russell Koffler and Mr. Charles Earnest for computer assistance and to Messrs. Clyde Jones and John Hildebrand who prepared many charts and figures.

REFERENCES

1. C. L. Bristor, W. M. Callicott, and R. E. Bradford, "Operational Processing of Satellite Cloud Pictures by Computer," *Monthly Weather Review*, vol. 94, No. 8, Aug. 1966, pp. 515–527.
2. E. B. Fawcett and H. K. Saylor, "A Study of the Distribution of Weather Accompanying Colorado Cyclogenesis," *Monthly Weather Review*, vol. 93, No. 6, June 1965, pp. 359–367.
3. S. Fritz and J. S. Winston, "Synoptic Use of Radiation Measurements From Satellite TIROS II," *Monthly Weather Review*, vol. 90, No. 1, Jan. 1962, pp. 1–9.
4. W. H. Klein, "Specification of Precipitation from the 700-Millibar Circulation," *Monthly Weather Review*, vol. 91, Nos. 10–12, Oct.–Dec. 1963, pp. 527–536.
5. W. H. Klein, C. W. Crockett, and J. F. Andrews, "Objective Prediction of Daily Precipitation and Cloudiness," *Journal of Geophysical Research*, vol. 70, No. 4, Feb. 15, 1965, pp. 801–813.
6. E. N. Lorenz, "Empirical Orthogonal Functions and Statistical Weather Prediction," *Scientific Report No. 1, Statistical Forecasting Project*, Dept. of Meteorology, Massachusetts Institute of Technology, Cambridge, Mass., 1956, 49 pp.

7. E. P. McClain, M. A. Ruzecki, and H. J. Brodrick, "Experimental Use of Satellite Pictures in Numerical Prediction," *Monthly Weather Review*, vol. 93, No. 7, July 1965, pp. 445–452.
8. R. G. Miller, "The Screening Procedure, Part II of Studies in Statistical Weather Prediction," Final Report, Contract No. AF19(604)–1590, Travelers Weather Research Center, Hartford, Conn., 1958, pp. 86–136.
9. P. K. Rao and J. S. Winston, "An Investigation of Some Synoptic Capabilities of Atmospheric Window Measurements from Satellite TIROS II," *Journal of Applied Meteorology*, vol. 2, No. 1, Feb. 1963, pp. 12–23.
10. P. E. Sherr and R. Wexler, "Operational Use of TIROS Radiation Measurements," Final Report, Contract No. AF 19(628)–4074, ARACON Geophysics Co., Concord Mass., 1965, 51 pp.
11. W. K. Widger, Jr., J. C. Barnes, E. S. Merritt, and R. B. Smith, "Meteorological Interpretation of Nimbus High Resolution Infrared (HRIR) Data," Final Report, Contract No. NAS5–9554, ARACON Geophysics Co., Concord, Mass., 1965, 222 pp.
12. J. S. Winston, "The Operational Use of Meteorological Satellite Data," *Annals of New York Academy of Science*, vol. 93, 1962, pp. 775–812.
13. J. S. Winston, "Global Distribution of Cloudiness and Radiation for Seasons as Measured from Weather Satellites," (to be published in vol. 3, *Climate of the Free Atmosphere*, of the *World Survey of Climatology*, Elsevier Publishing Co., Amsterdam, 1966).

[*Received July 15, 1966; revised September 13, 1966*]